

# Microfracture Strength Evaluation Technique Using Nano-polycrystalline Diamond Spherical Indenter

Hitoshi SUMIYA\*, Kensei HAMAKI, and Katsuko HARANO

We have developed a microfracture strength evaluation technique that uses a spherical indenter made from nano-polycrystalline diamond. The technique enables us to evaluate the fracture strength characteristics in the micro regions of diamond materials with a high accuracy, which has been difficult in the past. Through evaluation tests on various types of single crystal diamonds using the technique, it was revealed that the fracture strength of natural diamond greatly differs depending on the location in each crystal, while that of synthetic diamond is uniform with small deviations. We also confirmed that the microfracture strength of nano-polycrystalline diamond is increased through grain refinement.

Keywords: diamond, microfracture strength, nano-polycrystal, single-crystal, indenter

## 1. Introduction

Natural and synthetic single-crystal diamonds (SCDs) have been widely used as materials for machining tools such as high-precision bits, cutters, dressers, and dies. Recently, ultra-hard nano-polycrystal diamond (NPD), which has higher hardness and strength than those of SCD, has been newly developed by direct conversion sintering at ultra-high pressure. NPD has been commercialized as precision machining tools for hard and brittle materials such as cemented carbide and hard ceramics.<sup>(1),(2)</sup> Nano-polycrystal cubic boron nitride (cBN) has also been developed by a similar process and used for cutting tools of ferrous materials.<sup>(2)</sup>

To apply these hard diamond materials to machining tools, it is essential to fully understand their mechanical characteristics. For cutting tools such as precision bits and cutters in particular, the fracture strength, which is related to the chipping resistance of tools, is an important factor that determines the performance. Notably, the fracture strength in the micro region (microfracture strength), which corresponds to microchipping at the blade tip during cutting, is important. However, diamond materials are very hard and brittle, and therefore it is extremely difficult to quantitatively evaluate their fracture strength. The transverse rupture strength (TRS)\*<sup>1</sup>, which is commonly used to evaluate the fracture strength of ceramic and metallic materials, is difficult to measure for diamond materials due to the specimen size and workability, and the fracture strength in microscopic regions cannot be evaluated.

In order to evaluate the microfracture strength of diamond materials, we developed a simple and high-precision evaluation technique based on the Hertzian fracture test,<sup>(3)</sup> which is used to evaluate the fracture strength of brittle materials such as glass. In this method, a spherical NPD indenter is indented onto a specimen, and the load at which a crack is generated due to elastic deformation is used as an index of fracture strength (crack resistance). The key to this evaluation technique is the use of an NPD, which has high strength and isotropic mechanical characteristics, as an indenter. This enables accurate and simple evaluation of the microfracture strength without fracture of

an indenter on diamond-related materials. Using this evaluation technique, we demonstrated that the fracture strength of natural SCDs differs significantly depending on the crystal or the position in the same crystal, while the difference in fracture strength is small for synthetic SCDs. We also confirmed that high-quality synthetic SCDs characterized by high purity and few defects are particularly stable. Regarding NPDs and nano-polycrystal cBN, it was found that the finer the structure, the higher the microfracture strength, resulting in improved crack resistance.

## 2. Development Concept

The conceptual diagram of the Hertzian fracture test<sup>(3)</sup> is shown in Fig. 1. In this test, a spherical indenter is pressed onto a specimen to generate ring cracks due to the tensile stress caused by elastic deformation. The physical value of fracture strength can be calculated from the crack initiation, size of the ring crack, and mean pressure on the contact surface. This method is used to evaluate the fracture strength of brittle materials such as glass and ceramics. Usually, a hard steel ball or spherical ceramic body is used as an indenter.

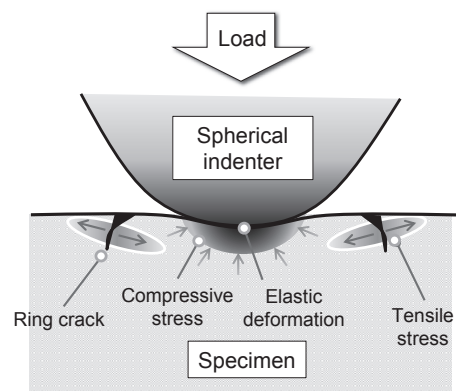


Fig. 1. Fracture strength test using a spherical indenter (Hertzian fracture test)

A microfracture strength test of SCD specimens using this method was reported previously.<sup>(4),(5)</sup> In the test, a conical SCD indenter with a spherical tip was used. However, it is difficult to fabricate a spherical indenter with adequate sphericity because the abrasion characteristics of SCD significantly differ depending on the crystal orientation. Inadequate sphericity of an indenter leads to an inaccurate value of the crack initiation load, resulting in poor reproducibility. Another significant issue is that SCD spherical indenters are likely to be damaged due to cleavage. Notably, SCD indenters are easily broken when a fracture strength test is conducted on ultra-hard NPD specimens.

The Knoop hardness of SCD varies greatly from 70 to 125 GPa depending on the surface orientation,<sup>(6)</sup> whereas the Knoop hardness of NPD is high at around 130 GPa and entirely isotropic.<sup>(7)</sup> NPD is characterized by extremely high wear resistance and free from the anisotropy that is a characteristic of SCD.<sup>(8)</sup> In addition, NPD is free from cleavage due to the polycrystalline structure, and so their TRS is higher than that of SCD.<sup>(2)</sup> Figure 2 shows a comparison of characteristics between NPD and SCD. We assumed that the microfracture strength characteristics of diamond materials such as SCD and NPD would be accurately evaluated by using an NPD that has high hardness, high strength, and isotropic mechanical characteristics as a spherical indenter to avoid damage. Thus, we fabricated a prototype spherical indenter using an NPD to develop a microfracture strength evaluation technique.



	Single-crystal (SCD)	Nano-polycrystal (NPD)
		
Grain size	-	30-50 nm
Knoop hardness	RT	70-125 GPa
	800°C	50-60 GPa
TRS	1-2 GPa	3-5 GPa
Isotropy	Anisotropic	Isotropic
Cleavage feature	(111) cleavage	No cleavage

Fig. 2. Characteristics of SCD and NPD

### 3. Development of a New Evaluation Technique

#### 3-1 Fabrication of NPD spherical indenters

NPD samples were synthesized by direct conversion (pressure: 16 GPa, temperature: 2,300°C) using high-purity graphite as the starting material.<sup>(1),(2)</sup> The NPD samples were machined into discs measuring  $\phi 1-1.5$  mm by surface grinding and laser cutting and brazed onto holders. A diamond grinding wheel was used to form conical indenters (cone angle: 120°) with a spherical tip. The indenter surface was polished (mirror-finished) with the surface

roughness (Ra) of 30 nm or less using a diamond wheel with fine grains. The spherical part at the tip of the obtained NPD spherical indenters ( $R = 50 \mu\text{m}$ ) was characterized by satisfactory surface accuracy and sphericity, as shown in Fig. 3 (a). When SCDs were polished, the surface profile was distorted into an almost square shape due to uneven abrasion<sup>(8)</sup> (see Fig. 3 (b)). Thus, highly spherical and high-precision indenters can be formed from NPDs as described above due to their isotropic mechanical characteristics.<sup>(8)</sup>

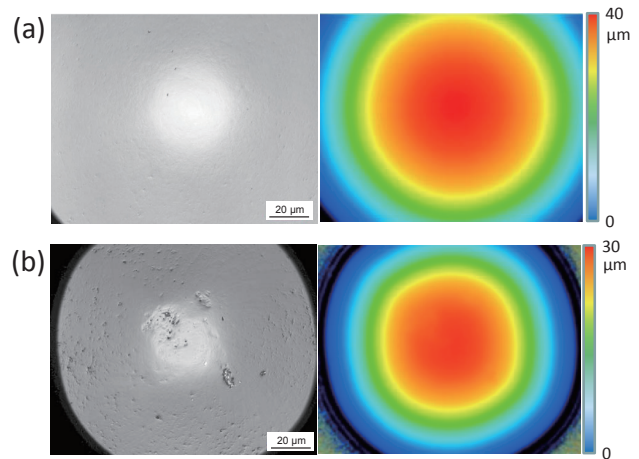


Fig. 3. Optical microscope image of spherical indenters and surface profile obtained by a laser scanning microscope. (a) NPD spherical indenter, (b) SCD spherical indenter

#### 3-2 Method of evaluating microfracture strength

Next, the method of evaluating microfracture strength using the NPD spherical indenters is discussed. Figure 4 shows a schematic drawing of the evaluation method. An NPD spherical indenter was pressed onto a specimen, and the load was continuously increased at the rate of 1 N/s

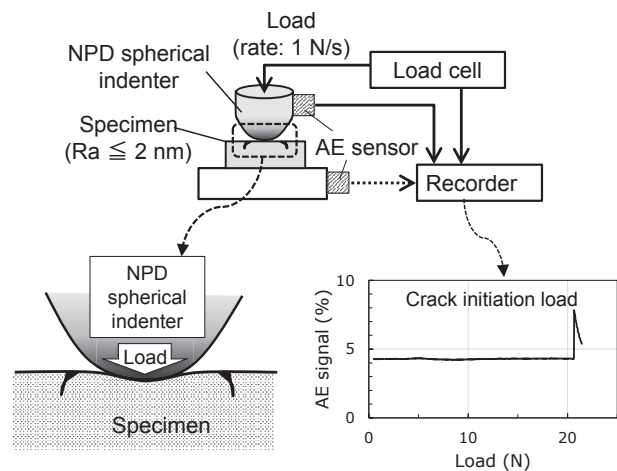


Fig. 4. Evaluation of the microfracture strength characteristics (crack resistance) by measuring the crack initiation load

using a load controller. A ring crack was generated by the tensile stress outside the contact area. An acoustic emission (AE)\*<sup>2</sup> sensor was used for detection to measure the crack initiation load.

If the radius of the NPD spherical indenter (R) is too small, plastic deformation is caused by excessive compressive stress and no ring crack due to tensile stress is observed. Figure 5 shows the cross-sectional data of impressions after indentation onto an NPD specimen with various NPD indenter radii (R), measured by using a 3D optical surface profiler. For NPD indenters whose R was 12  $\mu\text{m}$ , the surface of the NPD specimens was subject to plastic deformation (see (a)). For NPD indenters whose R was 55  $\mu\text{m}$ , no plastic deformation was observed and cracks due to tensile stress were generated (see (b)). We conducted experiments by changing the value of R and confirmed that no plastic deformation occurred on the NPD or SCD specimens when the indenter radius was approximately 30  $\mu\text{m}$  or more, and that the intended ring crack could be generated. We investigated the influence of the radius and surface condition of NPD spherical indenters and found that the crack initiation load of SCD and NPD specimens could be measured with an error of  $\pm 15\%$  or less by setting the value of R of an NPD indenter to  $50 \pm 5 \mu\text{m}$ . We also confirmed that an NPD indenter of this size was not damaged even after using it several hundred times on SCD and NPD specimens and that the surface profile showed little change.

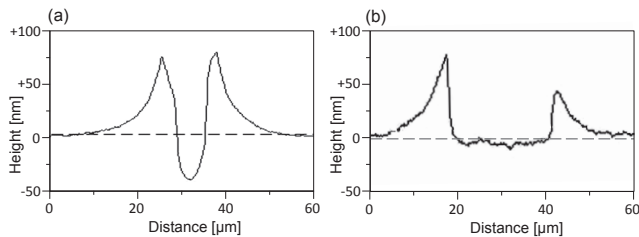


Fig. 5. Cross-sectional profile of impression after indentation on the surface of an NPD specimen using an NPD spherical indenter. Indenter radius (R): (a) 12  $\mu\text{m}$ , (b) 55  $\mu\text{m}$

Examples of ring cracks generated by indentation of an indenter (R = 50  $\mu\text{m}$ ) on SCD and NPD specimens are shown in Fig. 6. Cracks generated on the SCD (100) surface were rectangular along the direction of the intersection line with the (111) cleavage plane. On the (111) plane, hexagonal ring cracks were generated. In this way, no circular ring crack was generated on SCD specimens. By contrast, almost circular ring cracks were generated on NPD specimens because NPDs are polycrystalline substances and free from cleavage. However, the shape of the ring crack was often deformed slightly, and multiple circular cracks were generated in some cases. Thus, on diamond materials, it was difficult to identify the radius of the ring crack, although it is required to calculate the physical value of microfracture strength. Therefore, in this research, we used the crack initiation load value (N) as an index for the microfracture strength.

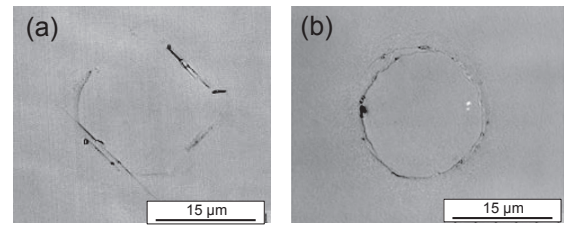


Fig. 6. Examples of ring cracks generated by indenting NPD spherical indenter of R=50  $\mu\text{m}$  onto (a) SCD and (b) NPD specimens

## 4. Evaluation Test on Various Diamond Materials

### 4-1 Single-crystal diamonds (SCDs)

The evaluation method mentioned above was used to evaluate three types of SCD specimens: a type Ia natural SCD, which is generally used for industrial applications (containing several hundreds to thousands of ppm of aggregated nitrogen impurities), a type Ib high-pressure synthetic SCD, which is manufactured by Sumitomo Electric Industries, Ltd. for tool materials (containing about 100 ppm of substitutional nitrogen impurities), and a type IIa high-pressure synthetic SCD, which was developed for research (containing 0.1 ppm or less of impurities).<sup>(9)</sup> The measuring plane was (100), which is not greatly affected by cleavage. The measuring plane of each specimen was polished in the  $\langle 110 \rangle$  direction using a diamond wheel, and the surface roughness was reduced to  $R_a \leq 2 \text{ nm}$  for the experiment.

The crack initiation loads of respective specimens were measured 10 times at different positions of 0.3–0.5 mm intervals. Figure 7 shows the mean values and deviations of the respective specimens. For the natural SCD, the crack initiation load was significantly varied (several times) depending on the specimens. For the high-pressure synthetic SCDs (types Ib and IIa), the difference between specimens was small as 10% or less. The value of the crack initiation load was highest for the high-pressure synthetic type IIa.

The difference by position in a single crystal is shown in Fig. 8. In the natural diamond, the crack initiation load

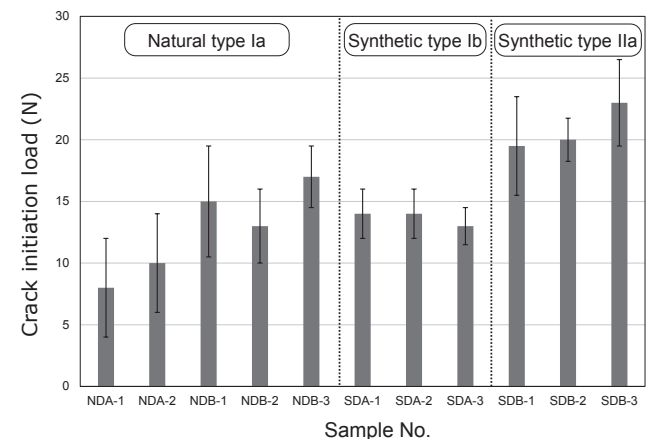


Fig. 7. Crack initiation load of each natural and high-pressure synthetic SCD

differs up to about six times depending on the crystal position. In contrast, the difference in the crack initiation load in a crystal of the high-pressure synthetic SCDs was smaller (about 10–20%) than that of the natural SCDs. We investigated the residual stress near the measurement point at the crack initiation load of respective diamond materials based on the shift of the Raman scattering spectrum, and found that the stress in the natural SCDs differed by about  $\pm 0.2$  GPa depending on the position. This internal stress is considered to cause a significant change in the crack initiation load. In the high-pressure synthetic SCDs, the distribution of the internal stress was  $\pm 0.01$  GPa or less, and no significant difference was observed. This seems to lead to the small deviation of the crack initiation load. However, when the high-pressure synthetic type Ib SCDs (generally manufactured for industrial applications) were evaluated at a fine pitch of about 0.1 mm, cracks were sometimes generated locally at a low load. This is attributable to the influence of the dislocation defects that spread from the seed crystal in the directions of  $\langle 001 \rangle$  and  $\langle 112 \rangle$ .<sup>(10)</sup> In other areas that had few defects, the fracture strength characteristics were stable. Notably, the synthetic type IIa SCD was characterized by very few crystal defects and internal distortion.<sup>(9)</sup> Thus, the overall crack initiation load was high, and the deviation was small.

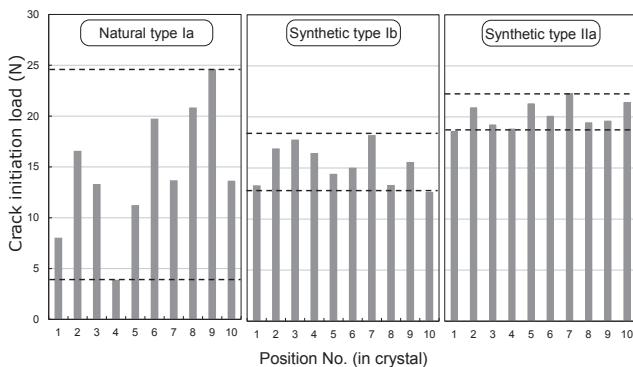


Fig. 8. Variation of crystal initiation load depending on the measured position in each crystal

#### 4-2 Nano-polycrystal diamonds (NPDs)

Nano-polycrystal diamonds (NPDs) of different grain sizes were synthesized by direct conversion at ultra-high pressure and high temperature using various types of graphite of different graphitization degree (P1)<sup>(11)\*3</sup> as the starting material. The crack initiation load of each specimen was evaluated by the same method described above. The measuring plane of each specimen was polished by a diamond wheel to attain the surface roughness of  $R_a \leq 2$  nm.

Table 1 shows the evaluation results of three types of NPDs obtained. The results clearly show that the smaller the grain size, the higher the crack initiation load, suggesting that the chipping resistance of the blade tip when used as a cutting tool would improve due to the decrease in grain size.

Table 1. Evaluation results of the crack initiation load of NPD specimens of different grain sizes

Specimen	NPD-A	NPD-B	NPD-C
NPD grain size (nm)	~ 100	~ 30	~ 10
Crack initiation load (N)	7	10	16

We also evaluated nano-polycrystal cBN derived from direct conversion at ultra-high high pressure and high temperature, and confirmed that the finer the structure, the higher the fracture strength, as in the case of NPDs.<sup>(12)</sup> The details are omitted in this report.

Thus, the microfracture strength test using an NPD spherical indenter makes it possible to clarify the influence of the microstructure of the superhard nano-polycrystal specimens on microfracture strength.

## 5. Conclusion

We developed a simple and highly accurate evaluation technique in which the crack initiation load is measured using spherical indenters fabricated from NPDs and the measurement results are used as indices of microfracture strength (crack resistance). This technique enabled us to quantitatively measure the fracture strength in the micro region of ultra-hard diamond-related materials that has been quite difficult to evaluate. We used the technique to evaluate various types of diamond materials, and found that the difference in the fracture strength in the natural SCDs is high (both between individuals and in a crystal) and that synthetic SCDs with few crystal defects have stable strength characteristics. We also found that in-depth evaluation in the micro region helps to investigate the distribution of microdefects in crystals. In addition, we could clarify that the crack resistance of NPDs can be improved by controlling microstructures. Thus, this evaluation technique is a useful alternative to evaluate the practical performance such as chipping resistance and mechanical wear resistance when diamond materials are used as tools. It is also effective when investigating the distribution of the strength characteristics in the micro region attributed to local structural defects and microinclusions and when elucidating the mechanism of fractures.



### Technical Terms

- \*1 Transverse rupture strength (TRS): An index of material strength calculated from the maximum load applied until a test piece fractures in a three-point bending test.
- \*2 Acoustic emission (AE): A phenomenon in which the elastic strain energy accumulated in a material is released as acoustic waves (acoustic emission [AE] waves) when a material is deformed or fractured.
- \*3 Graphitization degree (P1): The crystallinity of graphite based on the ratio of the turbostratic structure calculated from the X-ray diffraction of graphite.

### References

- (1) H. Sumiya, "Novel development of high-pressure synthetic diamond · Ultra-hard nano-polycrystalline diamond," SEI Technical Review, No. 74, (2012) 15-23
- (2) H. Sumiya, K. Harano, "Innovative Ultra-hard Materials: Binderless Nanopolycrystalline Diamond and Nano-polycrystalline Cubic Boron Nitride," SEI Technical Review, No. 82, (2016) 21-26
- (3) H. E. Powell, F. W. Preston, "Microstrength of glass," J. Amer. Ceram. Soc. 28 (1945) 145-149
- (4) N. Ikawa, S. Shimada, "Microstrength Measurement of Brittle Materials Utilizing Acoustic Emission Technique," Seimitsu Kikai, 48 (1982) 177-183
- (5) N. Ikawa, S. Shimada, "Microfracture of diamond as fine tool material," Annals of the CIRP, 30 (1982) 71-74
- (6) H. Sumiya, "Super-hard diamond indenter prepared from high-purity synthetic diamond crystal," Rev. Sci. Instrum., 76 (2005) 026112
- (7) H. Sumiya, T. Irifune, "Indentation hardness of nano-polycrystalline diamond prepared from graphite by direct conversion," Diam. Relat. Mater., 13 (2004) 1771-1776
- (8) H. Sumiya, K. Harano, "Distinctive mechanical properties of nano-polycrystalline diamond synthesized by direct conversion sintering under HPHT," Diam. Relat. Mater., 24 (2012) 44-48
- (9) H. Sumiya, N. Toda, Y. Nishibayashi, S. Satoh, "Crystalline perfection of high purity synthetic diamond crystal", J. Crystal growth, 178 (1997) 485-494
- (10) H. Sumiya, K. Tamasaku, "Large defect-free synthetic type IIa diamond crystals synthesized via high pressure and high temperature," Jpn. J. Appl. Phys. 51 (2012) 090102
- (11) B. E. Warren, "X-Ray Diffraction in Random Layer Lattices," Phys. Rev. 59 (1941) 693-698
- (12) H. Sumiya, K. Hamaki, K. Harano, "Strength properties and cutting performances of ultra-fine high-purity nano-polycrystalline diamond and cBN," Proceedings of 2017 JSPE Autumn Conference, B30 (2017) 115-116

**Contributors** The lead author is indicated by an asterisk (\*).

### H. SUMIYA\*

• Fellow  
Advanced Materials Laboratory  
Dr. Eng.



### K. HAMAKI

• Advanced Materials Laboratory



### K. HARANO

• Group Manager, Advanced Materials Laboratory

